Effects of hypoxia on glutamate-activated currents in horizontal cells of the goldfish (*Carassius auratus*) retina

Written by: Alexia Adamo
Supervisor: Dr. Michael Jonz

19/04/2022

Contents

Abstract

Neuronal survival relies upon oxygen availability. During states of low oxygen (hypoxia), electrical gradients across the cell membrane become dysregulated, causing a rise in intracellular Ca^{2+} and, ultimately, excitotoxic cell death. Some species, such as goldfish (*Carassius auratus*) demonstrate the ability to tolerate prolonged hypoxia exposure and resist damage by elevated intracellular Ca^{2+}. Previous studies have used horizontal cells (HCs) as model neurons to study neuroprotective systems in the retina. Although the precise cellular mechanisms are poorly understood, recent evidence indicates that hypoxia paradoxically increases intracellular Ca^{2+} in the presence of glutamate. Using whole-cell patch-clamp, I tested the effects of hypoxia on ion channel currents in isolated HCs to identify potential pathways of Ca^{2+} permeability during hypoxia. Upon application with glutamate, glutamate receptors produced an inward current at negative membrane potentials. These currents increased during application of hypoxic extracellular solution. Preliminary experiments on voltage-gated Ca^{2+} channels suggest an additional pathway for Ca^{2+} influx during hypoxia. These results support a potential neuroprotective effect in the retina, where hypoxia may produce inhibitory feedback onto photoreceptors via enhanced depolarization and Ca^{2+} influx in HCs. This study presents a starting point for more sophisticated studies investigating the neuroprotective mechanisms of the goldfish retina in hypoxia.

Introduction

Anatomy of the retina

The vertebrate retina has been coined an "approachable part of the brain" for its accessibility and ability to provide insights into the central nervous system (CNS). These insights are made possible, in part, by the role the retina plays in the conversion of light to an electrochemical signal, thus contributing to the visual processing of images (Dowling, 1987). Visual processing begins when light energy travels through the retina to initiate phototransduction in photoreceptors (PRs), inhibiting their continual release of glutamate onto second-order bipolar cells (BCs) and horizontal cells (HCs) (Hoon *et al.*, 2014). HCs are a group of interneurons found in the inner nuclear layer where they receive glutamatergic inputs from upstream PRs during periods of darkness (Poché & Reese, 2009). HCs respond to glutamate activation by producing an inhibitory feedback signal to nearby PRs, referred to as lateral inhibition; this represents the first level of visual processing and contributes to edge detection and colour opponency. (Ströh et al., 2018; Thoreson and Mangel, 2012). By way of this lateral processing, HCs can modulate neural signals received by BCs from upstream PRs. Similarly, amacrine cells (ACs) act as inhibitory modulators of synaptic transmission between BCs to retinal ganglion cells (RGCs). RGCs are the retina's output neurons; they receive signals from BCs and ACs to be sent to the brain's visual cortex via the optic nerve (Wässle, 2004). From the optic nerve, signals are transmitted to the visual cortex in the brain, where they will be encoded as images (Shekhar et al., 2016).

Horizontal cell connectivity and morphology

Horizontal cell bodies possess processes extending into the outer plexiform layer, and are connected in a sprawling lateral network via gap junctions (O'Brien et al., 2006; Kaneko, 1971).

Gap junction channels in HCs provide a direct pathway for electrical signalling between cells, allowing for intercellular communication and an increase in the size of the receptive field (Jonz & Barnes, 2007). PRs, defined further as rods and cones, synapse with HCs via synaptic invaginations where HC dendrites are opposed to PR synaptic ribbons. These ribbon structures are vital for the rapid transmission of signals and release of neurotransmitters to downstream neurons (Sakai & Naka, 1986; Schmitz, 2009). HCs, BCs, and PRs synapse together differently depending on the types of cells present: HC dendritic processes and ON-bipolar cell dendrites invaginate into the photoreceptor terminals to form a "triad" synapse, whereas OFF-bipolar cells make contact at the base of the photoreceptor terminal (Haverkamp *et al.*, 2000). The connections between these various cell types contribute to the modulation of sensory information which travels from the retina to the optic nerve.

Of HCs found in the teleost retina, there exist 4 subtypes. These subtypes have been labelled H1 through H4 and are characterized in order of increasing number of dendrites, decreasing size in the cell body, and increased distance from the outer retinal layer. Subtypes H1-H3 synapse specifically with cones of PRs, while the H4 subtype synapses with rods (Stell & Lightfoot, 1975). Each subtype is selectively excited by various wavelengths of light stimulus by their respective PRs, which elicit different cell responses--some of which are hyperpolarizing and others depolarizing, depending on the light signal being received (Perlman et al., 2012). Additionally, teleost HCs are characteristically large, making them ideal candidates for electrophysiological study. HCs were the first cells of the retina from which intracellular recordings were obtained (Dowling 1987; Svaetichin 1953). For these reasons, HCs share a long history as model central neurons and have been widely studied for over a century (Ramón y Cajal 1909).

The response to glutamate in the retina

The glutamate released from PRs binds to iGluRs on HCs, which include Ca^{2+} permeable and Ca^{2+} impermeable α-amino-3-hydroxy-5-methyl-4-isoxazole propionic acid receptor (AMPARs), kainate receptors (KARs), and NMDARs (Brandstätter et al., 1998). AMPARs often provide a fast postsynaptic response from presynaptic glutamate release, resulting in a quick activation of the receptor. The permeability of these receptors to Ca^{2+} is dependent on the presence of the GluA2 subunit (Gasbarri & Pompili, 2014). Like all iGluRs, kainate receptors depolarize neurons upon glutamate activation but differ in that they also exhibit metabotropic types (Bhangoo & Swanson, 2013). NMDARs are characterized by their high permeability to Ca^{2+} ions. Activation of these NMDA receptors via glutamate release causes membrane depolarization and a subsequent increase in intracellular Ca^{2+} ($[Ca^{2+}]_i$) (Yin Shen et al., 2006).

When glutamate binds to iGluRs, their opening allows for the nonspecific passage of cations. This is predominantly Na^+ and K^+ which results in the rapid depolarization of the cell and by consequence, the opening of VGCCs that allow entry of Ca^{2+} (Twomey & Sobolevsky, 2018). HCs undergo a response characterized by an initial, short-lived peak in $[Ca^{2+}]_i$ followed by a sustained increase in $[Ca^{2+}]_i$ via L-type voltage-gated Ca^{2+} channels (VGCCs) for the duration of glutamate application (Linn and Christenen, 1932; Palmer et al., 2005). The small amount of Ca^{2+} that enters the cell upon iGluR activation is sufficient to induce calcium-induced calcium release (CICR) from the endoplasmic reticulum (ER), where large amounts of sequestered and intracellular calcium are stored. This release of Ca^{2+} is mediated by ryanodine receptors (RyR) located in the ER membrane (del Prete *et al.*, 2014).

Horizontal cell mechanisms of inhibition

Lateral inhibition is the phenomenon in which HCs receive glutamatergic signals from upstream PRs in darkness and produce inhibitory feedback signals back onto the PRs to modulate downstream signalling onto BCs. However, the precise mechanism by which HCs produce this feedback is poorly understood and still under debate (Thoreson & Mangel, 2012). Three main hypotheses for HC inhibition have been considered: (1) release of inhibitory neurotransmitter GABA onto PRs, (2) a pH-dependent pathway and (3) an ephaptic mechanism.

According to the GABA hypothesis, glutamate released from PRs depolarizes HCs, which then release GABA back onto photoreceptors. Activation of GABA receptors hyperpolarizes the cone terminal, suppressing the activation of cone VGCCs and reducing glutamate release. A gap in this hypothesis has been identified by experiments that observed continued inhibition even after GABA receptor blockage, thereby disproving GABA as the central inhibitory mechanism. (Kramer & Davenport, 2015). Secondly, the proton hypothesis was developed following studies that have shown a proton-dependent mechanism of inhibition, in which HCs or regulate of synaptic cleft pH an shift the activation potentials of Ca^{2+} channels on PRs (Jacoby et al., 2012; Beckwith-Cohen et al., 2019). What remains unclear in this hypothesis is the mechanism that links HC voltage to changes in synaptic pH (Kramer & Davenport, 2015). Thirdly, in the ephaptic mechanism, feedback is created by the generation of current through the extracellular synaptic space, resulting in a voltage drop at the HC synapse (Byzov & Shura-Bura, 1986). Through the production of an external negative potential, Ca^{2+} channels located in the synaptic terminal of HCs will sense this voltage drop and decrease glutamate release (Barnes et al., 2020). Experiments have implicated connexin hemichannels in HC feedback; however, experiments that block these channels have presented mixed results (Kramer & Davenport, 2015). Although these feedback

mechanisms have been extensively studied, it is still unclear which mechanism is the correct one, further proving the importance of work in this field. A more recent study, however, presents the idea of a hybrid pH-GABA model of inhibitory feedback (Barnes *et al*. 2020).

Lateral inhibition sets the stage for antagonistic center-surround receptive fields exhibited in the visual system, an organizational feature in the retina, which contributes to high acuity vision by producing visual contrast. BCs are either considered to be ON-center or OFF-center based on their activation in light or darkness (Feher, 2012). OFF-center bipolar cells are excited in the *presence of* glutamate and are therefore active when the light is off at their center. In contrast, ON-center BCs are *inhibited* by the release of glutamate. Thus, once light is present, PRs are hyperpolarized, releasing less glutamate, and ON-center BCs are activated while OFF-center BCs are downregulated (Snellman *et al.*, 2008). In areas of the receptive field where light is present, HCs will be downregulated and therefore minimize their inhibitory effects. Conversely, in areas of darkness, HCs will be activated and increase inhibition on PRs, therefore amplifying the signal where the stimulus is strongest (Byzov & Trifonov, 1968). The lateral inhibitory effects produced by HCs in turn govern the antagonistic surrounding receptive field of downstream BCs (Yang & Wu, 1991). This characteristic center-surround arrangement of cells, made possible by lateral inhibition, is seen throughout the layers of the retina and contributes greatly to edge detection and visual processing of colour (Ankri *et al.*, 2020).

Consequences of hypoxia and neuroprotective mechanisms

The maintenance of electrical gradients across the cell membrane is an energetically costly activity that consumes over 50% of a neuron's ATP (Ames, 2011). Oxygen is essential for cell survival and is considered the primary energy molecule of life. When oxygen levels become

suboptimal (hypoxia) aerobic ATP production halts and the cell must rely upon anaerobic ATP production, which only produces 1/10 of the ATP that would be produced in aerobic conditions. In hypoxia, when ATP production and availability are reduced, dysregulation of the electrical gradient across the cell membrane ensues, shutting down the Na^+/K+ ATPase and reducing its ion shuttling capacity. As a result of the dysregulation of transmembrane ion gradients, $[Ca^{2+}]_i$ rises through influx in VGCCs and iGluRs (Berliocchi et al., 2005; Pál et al., 2020). In the wake of insufficient ATP, the cell becomes unable to repolarize the membrane or pump out increasing $[Ca^{2+}]_i$. This causes an accumulation of extracellular glutamate, which activates glutamate receptors even further (Papazian *et al.*, 2018). Much like in a typical glutamate response, depolarization via glutamate receptor activation triggers an increase in Ca^{2+} through activation of iGluRs and predominantly through the opening of VGCCs (Hayashida & Yagi, 2002). However, the dysregulation of glutamate release causes a sustained Ca^{2+} influx into the cell (Mehta *et al.*, 2013). A resulting constant influx of Ca^{2+} induces downstream neurotoxic effects, such as mitochondrial dysfunction, an increase in production of reactive oxygen species (ROS) and promotion of apoptosis (Armada-Moreira *et al.*, 2020). The increased activation of glutamate receptors continues to promote increased Ca^{2+} influx, which can reach levels high enough to be toxic to the cell, ultimately initiating the process of cell death; a process referred to as excitotoxicity (Bickler & Buck, 1998). Such dysregulation of intracellular Ca^{2+} can have profound system-wide effects and are a major contributor to neurogenerative diseases such as Alzheimer's and Parkinson's disease (Dong *et al.*, 2009).

Unlike terrestrial species, aquatic animals, such as fish and amphibians, are often exposed to varying oxygen availabilities underwater, such as overwintering under ice sheets, or varying oxygen levels caused by organic decay and eutrophication. Consequently, many aquatic species

have adapted to hypoxic or even anoxic conditions without long-lasting adverse effects (Hermes-Lima & Zenteno-Savín, 2002; Bickler & Buck, 2007). A prominent example of tolerance can be seen in the western painted turtle *(Chrysemys picta*)—the most anoxia-tolerant tetrapod. This species can survive for 4 months in anoxic conditions, most likely made possible by metabolic suppression to near-comatose levels (Keenan *et al.*, 2015). Studies performed on Crucian carp (*Carassius carassius)* using electroretinogram responses to light showed that vision "turns off", both within the retina and optic tectum, during anoxia but is then restored once returned to normoxic conditions (Johansson *et al.*, 1997). This restoration of vision suggests a hypoxia-tolerant mechanism in the eye, but the cellular mechanism by which this is achieved has not been investigated extensively in the retina.

The common goldfish (*Carassius auratus*) is yet another hypoxia tolerant species with mechanisms to survive in low oxygen conditions. Goldfish can survive hypoxia for long periods at varying temperatures; 45 hours under anoxic conditions at 5°C and 22 hours at 20°C; by decreasing their metabolic activity (Bickler & Buck, 2007). Studies conducted by Nilsson et al. in 2001 further characterized additional methods of tolerance exhibited by *Carassius* spp. such as "channel arrest"; wherein ATP supply in the brain is conserved by inhibiting the function of ion channels in the cell membrane (Hochachka, 1986). This phenomenon can be seen in neurons of the freshwater turtle, where permeability to Ca^{2+} ions decreases to avoid possible harmful accumulation (Nilsson, 2001; Bickler & Buck, 1998). Furthermore, *C. auratus* demonstrate mitochondrial ATP-dependant K^+ channel (mK_{ATP}) activation to stabilize baseline $[Ca^{2+}]_i$ during hypoxia to aid in preventing excitotoxic cell death (Country and Jonz, 2021). Based on the common goldfish's ability to withstand hypoxia, they are widely used as experimental models to study the mechanisms by which this species can survive in such conditions (Filice *et al.*, 2020)

Given the previously outlined relationship between hypoxia and glutamate receptor activation, this study aimed to explore the effects of hypoxia on glutamate-activated currents in isolated horizontal cells of the goldfish retina. Unpublished Ca^{2+} imaging work from the Jonz lab suggests that hypoxia may be causing an increase in intracellular Ca^{2+} during the activation of glutamate receptors (Nagy, unpublished). Based on this finding, it is hypothesized that hypoxia will significantly increase glutamate-activated currents in isolated HCs. Furthermore, the effects of hypoxia on Ca^{2+} currents in isolated HCs will also be analyzed. I hypothesized that Ca^{2+} currents will increase, based on their increased intracellular levels in the presence of glutamate as seen in Ca^{2+} imaging work. Using whole-cell patch-clamp, isolated HCs will be perfused with 100 μM glutamate in normoxic and hypoxic solutions to better understand the current-voltage relationship under these conditions. This study will provide further insight into how horizontal cells communicate with photoreceptors under hypoxic conditions. Further, examination of hypoxia tolerant mechanisms in the goldfish retina may inform future studies on medical conditions, such as diabetic retinopathy and stroke, both of which are diseases caused by insufficient oxygen availability to cells (Osborne et al., 2004; Hayreh & Zimmerman, 2005).

Materials and Methods

Animals

Adult goldfish (*C. auratus*) 8-13 cm in length were obtained from Aquality Tropical Fish supply Inc. Mississauga, Canada and maintained in a 270 L aquarium at 18°C on a 12 h:12 h light-dark cycle. All procedures for animal handling were performed in adherence to Canadian Council on Animal Care (CCAC). Goldfish were dark-adapted for 1 h during the day, before sacrifice and removal of the retina from the eyes.

Isolated horizontal cell preparation

Goldfish were stunned by a sharp blow to the head and pithed. Eyes were quickly removed and placed in cold Ca^{2+}-free Ringer's solution, containing the following (mM): 120 NaCl, 2.6 KCl, 0.5 NaH_2PO_4, 10 HEPES and 16 Glucose at pH 7.8. The eyes were hemisected to remove the sclera and lens, which allowed for access to the retinal layer. Retinas were carefully removed from the eyecup and placed into 100 U ml^{-1} hyaluronidase in L-15 solution for 20 min at room temperature. L-15 solution was made up of 30% Ca^{2+}-free Ringer's solution and 70% L-15 (Corning) (Connaughton & Dowling, 1998). Retinas were washed 3 times in fresh L-15 solution and then placed in papain solution containing 50.7 µl papain (Cat. no. LS003126, Worthington Biochemical Corporation, Lakewood, NJ, USA) and 2.5 mM cysteine (Fisher Scientific) for 40 min at room temperature. Retinas were washed another 3 times with fresh L-15 solution and left in the same solution until needed. HC isolation was done by triturating a small (approx. 2 mm) piece of tissue in L-15 solution with a glass Pasteur pipette and placing ~100 µl of cell suspension

in a 35 mm plastic Petri dish. Cells were allowed to settle for 10-15 min before patching. HCs were visualized using an inverted microscope (Leica).

Patch-clamp recording

Cells were clamped using whole-cell patch-clamp techniques. Electrodes were made using capillary glass (PG52151-4, World Precision Instruments Inc, Sarasota, Florida, USA) and pulled with a vertical pipette puller (model PC-10, Narishige CO. Ltd, Japan). Electrodes were fire-polished with a microforge (model MF-830, Narishige CO Ltd., Japan). Electrodes had a resistance of 4-8 MΩ when filled with intracellular recording solution containing (mM): 120 KCl, 10 NaCl, 0.5 $CaCl_2$, 2 Mg-ATP, 5 EGTA, 10 HEPES, pH adjusted to 7.4 with KOH. Voltage-clamp protocols were performed using an Axopatch-1D amplifier and pCLAMP7 (Axon instruments). Recordings were converted using a Digidata 1200 (Axon Instruments). Patched cells were recorded at -60 mV and then changed to various values of membrane potential (V_m). A voltage-step protocol was used to change potentials for 100 ms at a frequency of 100 Hz. Membrane capacitance was recorded using the Axopatch-1D amplifier. All data were analyzed using pCLAMP software and Prism 7.0. Figures were made using Prism 7.0 and Origin 7.0.

Experimental procedures and perfusates

Petri dishes were fitted with a superfusion chamber to allow for continuous flow of extracellular recording solutions in a small bath volume (200–300 µl) by gravity inflow (~2ml min^{-1}) and perfusion pump. Solutions were perfused into the recording chamber using a gravity-fed superfusion system. Changes in ion channel current were measured 2–3 min following application of the perfusates to ensure enough of the solution reached the bath. Patch-clamp

experiments were performed to show the potential effect of hypoxia on glutamate-activated currents. Recordings were obtained initially using extracellular solution (ECS) as a control (hypoxic ECS or normoxic ECS), depending on the experiment being performed. Solutions were made hypoxic by pumping 100% NO_2 to cause bubbling in solution reservoirs; hypoxic solutions were considered sufficiently hypoxic once bubbled for at least 15 min. Experiments designed to examine glutamate-activated currents prepared a normoxic and hypoxic solution of 100 μM glutamate (Fisher Scientific). Experiments designed to test Ca^{2+} channel currents utilized normoxic ECS and hypoxic ECS without glutamate. The hypoxic solution was made hypoxic in the same fashion.

Statistical analysis

All statistics are shown using either +/- S.E.M, and mean within the interquartile range. Differences in current density were compared using an unpaired t-test and nested t-tests. Statistical analysis was performed using Excel (Microsoft, Redmond, WA, USA) and Prism 7.0.

Results

Characterization of HCs in vitro

The goldfish retina's horizontal cells (HCs) were identified *in vitro* and recognized by their larger cell body and multiple dendritic processes. The experiments described investigated all HC subtypes; however, most subtypes in the experiments included subtypes H1 and H2. The average membrane capacitance (C_m) of HCs was 16.8 +/- 4 pF (n=11). During voltage-clamp recording, isolated HCs displayed a variety of membrane currents evoked by hyperpolarizing or depolarizing protocols from a holding potential of −60 mV (Fig. 1A). Potassium inward rectifying currents (I_{kir}), Ca^{2+} currents (I_{Ca}), and hemichannel currents (I_{γ}) were seen, similar to currents previously described (Tachibana, 1983). An I–V curve (Fig. 1B) was generated from these currents that closely resembles an 'N-shaped' curve, a characteristic I-V shape that has been previously described (Jonz & Barnes, 2007; Tachibana, 1983; Shingai & Christensen, 1986). Currents recorded from HCs were characterized by prominent inward current seen at voltages more negative than −80mV, a negative slope conductance between −70 and −40 mV and a sustained inward current that was activated near −40 mV and peaked between 0 and 10 mV, and outward rectification at voltages positive to 40 mV (Fig. 1 A and B).

Effects of hypoxia on glutamate-activated currents in HCs

Horizontal cell membrane currents have been previously shown to respond to the application of the excitatory neurotransmitter, glutamate (Tachibana, 1985). Both normoxic and hypoxic solutions containing 100 μM of glutamate were applied to isolated horizontal cells, and their effects on current were observed, as shown in Figure 2. The application of glutamate in normoxia and hypoxia had similar effects, in that both elicited an increase in inward current within

the physiological range (-70 mV to -20 mV). Additionally, glutamate application caused an increase in inward current at more negative voltages (-80 mV), while also increasing outward current at more positive voltages (+40 mV). Upon application of wash perfusate, the glutamate-activated response in HCs was attenuated and returned close to control values, further proving that the cell did respond to glutamate.

As seen in Figure 3A, glutamate-activated currents (demonstrated as current density) were shown to increase significantly in comparison to their respective controls under normoxic and hypoxic conditions, at a chosen voltage of -80 mV ($P<0.05$). The value of -80 mV was chosen for all statistical analyses since inward current peaks were consistent at this voltage, similar to the peak voltage described previously (Jonz & Barnes, 2007). It can be speculated that this peak was seen due to activation of glutamate receptors upon glutamate administration. As seen in Figure 3B, in comparison to normoxia, hypoxia increased glutamate-activated currents significantly ($P = 0.0075$). By comparing the difference in glutamate currents under both hypoxic and normoxic conditions (glutamate current-control current), the current density of cells exposed to hypoxia in glutamate is larger and more negative, indicating increased inward current. In addition, it was observed that in all experiments under hypoxic conditions, a noticeable variance can be seen in the values collected for glutamate in hypoxia, and hypoxia wash (Figure 3A). In contrast, the values plotted for experiments done in normoxia are less variable and appear more consistent.

Effects of hypoxia on Ca^{2+} *currents in HCs*

Sustained inward currents in HCs that activated near −40 mV (Fig. 1A and B) were inhibited by Cd^{2+} (Figure 4) and were characteristic of currents produced by Ca^{2+} ions through voltage-gated calcium channels, as previously described (Takahashi *et al.*, 1993). Ca^{2+} currents in

goldfish HCs were not significantly increased by administration of hypoxic perfusate. In a cell stepped from -60mV to various voltages (as shown in Figure 5A), I_{Ca} increased in hypoxia in comparison to I_{Ca} in normoxia (Figure 5), however, we did not find this increase to be considered significant ($P>0.05$). This same pattern occurred in one other cell but could not be replicated in the third cell of the sample size ($n=3$). Peak Ca^{2+} currents occurred between 0 and 10 mV, and the peak current within this range was used for statistical analysis (Figure 6). In addition, near the end of experiments in all 3 cells, some noticeable run down can be seen in the K_{ir} currents. This can be expected, as these channels have declining activity after being isolated from tissue.

Figure 1. Membrane currents in horizontal cells

A, patch-clamp recording shows membrane currents of a horizontal cell in extracellular solution at varying voltage steps (see figure) from a holding potential of -60 mV. ***B***, Representative current-voltage (I-V) relationship showing the membrane currents as a function of voltage steps in *A*. An "*N"* shape of the curve is produced by inwardly rectifying K^+ currents (I_{Kir}) below -80 mV, inward Ca^{2+} currents (I_{Ca}) from -40 mV to approximately 20 mV, and outward rectification above 40 mV due predominantly to hemichannel current (I_Y).

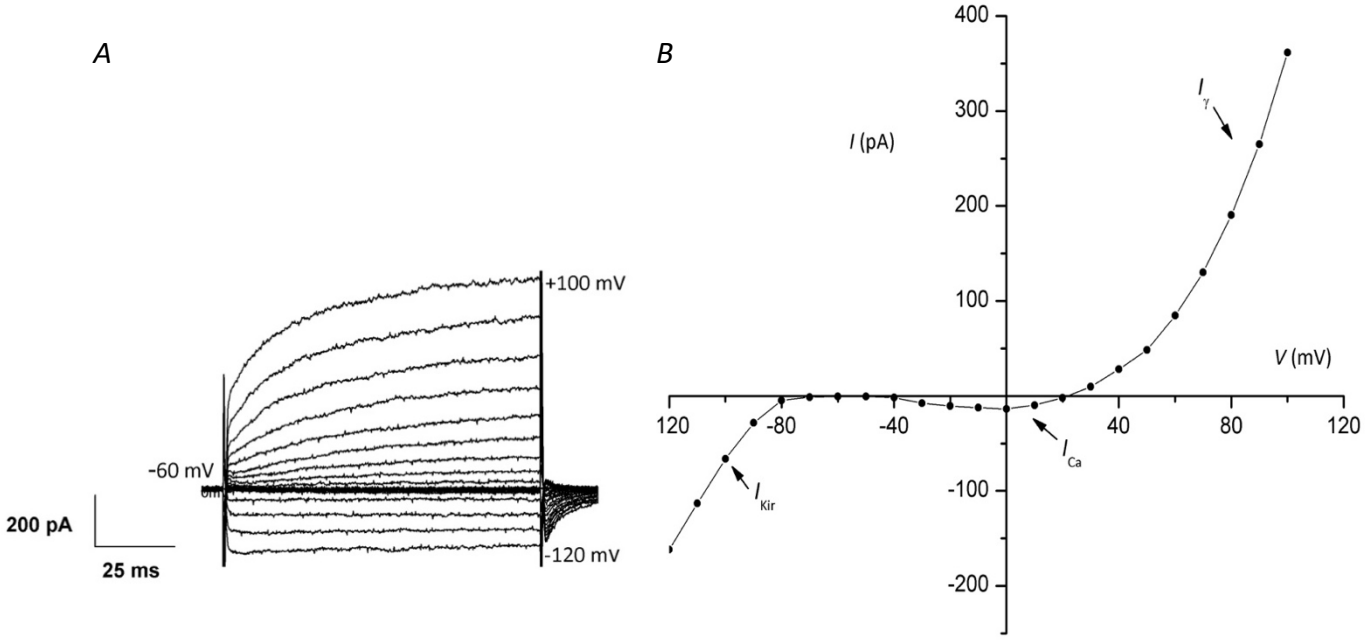
A
+100 mV
-60 mV
-120 mV
200 pA
25 ms
B
I (pA)
V (mV)
400
300
200
100
-100
-200
120
-80
-40
40
80
120
I γ
I Ca
I Kir

Figure 2. Current-voltage (I-V) relationship of glutamate-activated currents in horizontal cells in hypoxic vs. normoxic conditions

A, In a cell that was stepped from -60 mV to various voltages (see figure), inward currents and outward currents markedly increased compared to control upon administration of 100 μM glutamate. This glutamate response was attenuated by wash with control solution. ***C,*** the same cell was then subject to glutamate application in hypoxia. Like the normoxic condition, inward currents and outward currents increased in comparison to hypoxia control and were reversed by hypoxia wash. ***B***, ***D,*** I-V relationships of the recordings from the cell in *A* in normoxia and *C* in hypoxia, respectively. The effects of glutamate are seen via increased inward and outward rectifying currents and increased current within the physiological range (i.e., -80 mV to -20 mV). As in *A* and *C*, wash with control solution in normoxia or hypoxia reversed the effects of glutamate application.

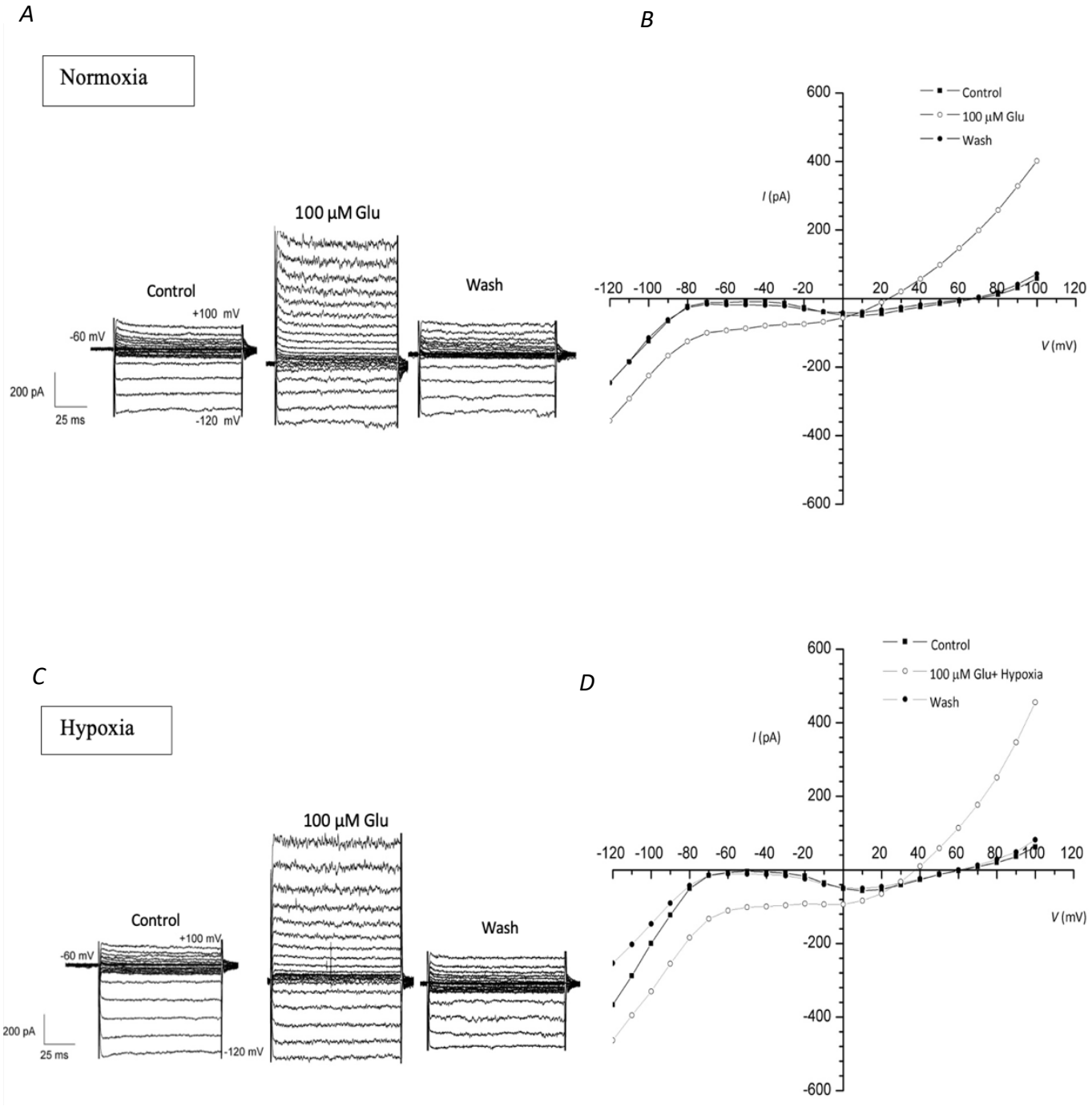
A
Normoxia
100 µM Glu
Control
Wash
+100 mV
-60 mV
-120 mV
200 pA
25 ms
B
Control
100 µM Glu
Wash
I (pA)
V (mV)
600
400
200
-200
-400
-600
-120 -100 -80 -60 -40 -20 20 40 60 80 100 120
C
Hypoxia
100 µM Glu
Control
Wash
+100 mV
-60 mV
-120 mV
200 pA
25 ms
D
Control
100 µM Glu+ Hypoxia
Wash
I (pA)
V (mV)
600
400
200
-200
-400
-600
-120 -100 -80 -60 -40 -20 20 40 60 80 100 120

Figure 3. Glutamate-activated currents are increased in hypoxia

A, Summary data of HC ion currents plotted as current density (pA/pF) in normoxia (n=8) and hypoxia (n=7). Values are presented as means +/- S.E.M. When cells were exposed to 100 μM glutamate, current density significantly increased in both hypoxia and normoxia compared to controls, as denoted by an asterisk in each panel ($P<0.05$; nested t-test). ***B,*** Summary data of difference currents (glutamate – control) in hypoxia and normoxia. A larger difference current was seen in hypoxia in comparison to normoxia, as denoted by the asterisk ($P<0.05$). An unpaired t-test was used to confirm the significance between the two groups.

A

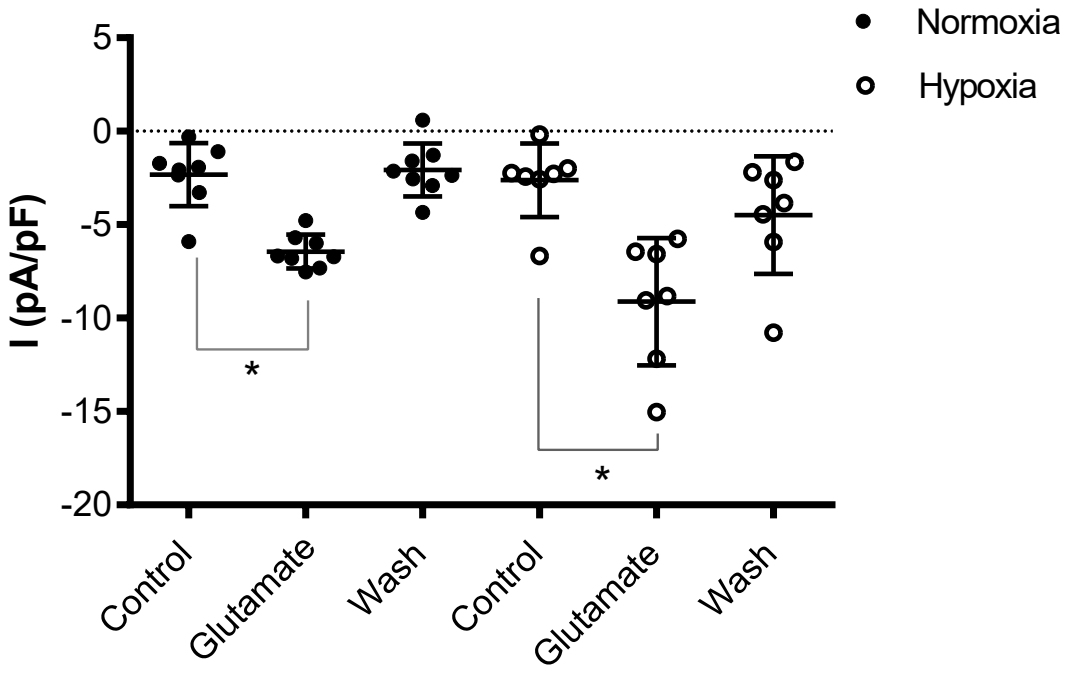
Normoxia
Hypoxia
I (pA/pF)
5
0
-5
-10
-15
-20
*
*
Control
Glutamate
Wash
Control
Glutamate
Wash

B

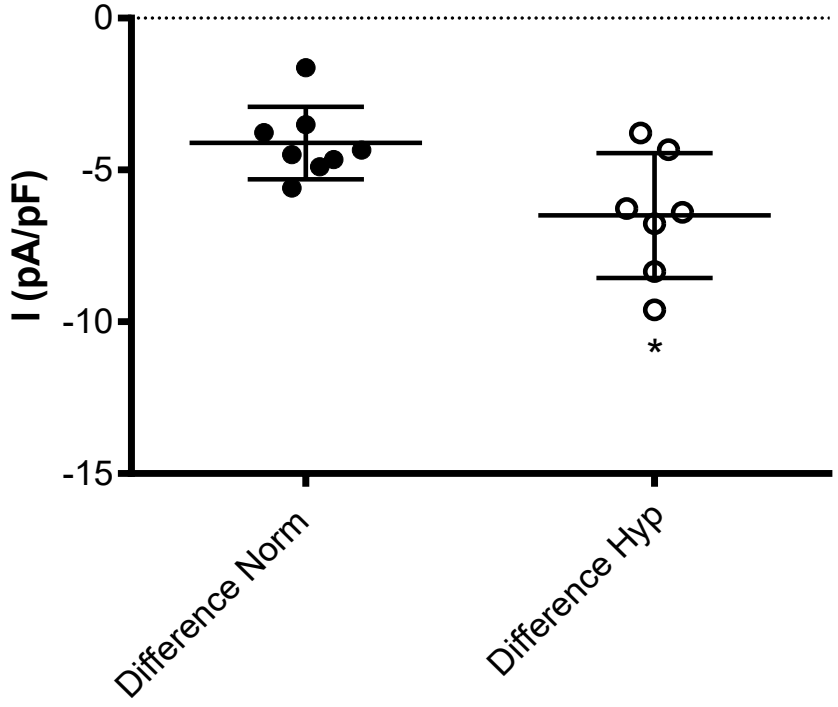
I (pA/pF)
0
-5
-10
-15
*
Difference Norm
Difference Hyp

Figure 4. Ca^{2+} channels were inhibited by Cd^{2+}

A, patch-clamp recording shows membrane currents of a horizontal cell upon administration of calcium channel blocker, Cd^{2+}, at a concentration of 50 μM at varying voltage steps (see figure). ***B,*** I-V relationship from isolated HC in *A,* showing attenuation of I_{Ca} by the Cd^{2+}. I_{Ca} of this cell was inhibited between -50mV and +10mV

A

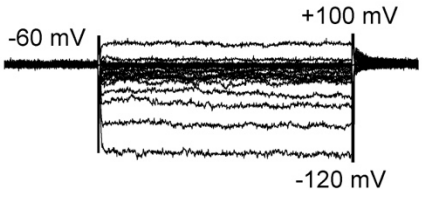
50 µM Cd2+
+100 mV
-60 mV
-120 mV

B

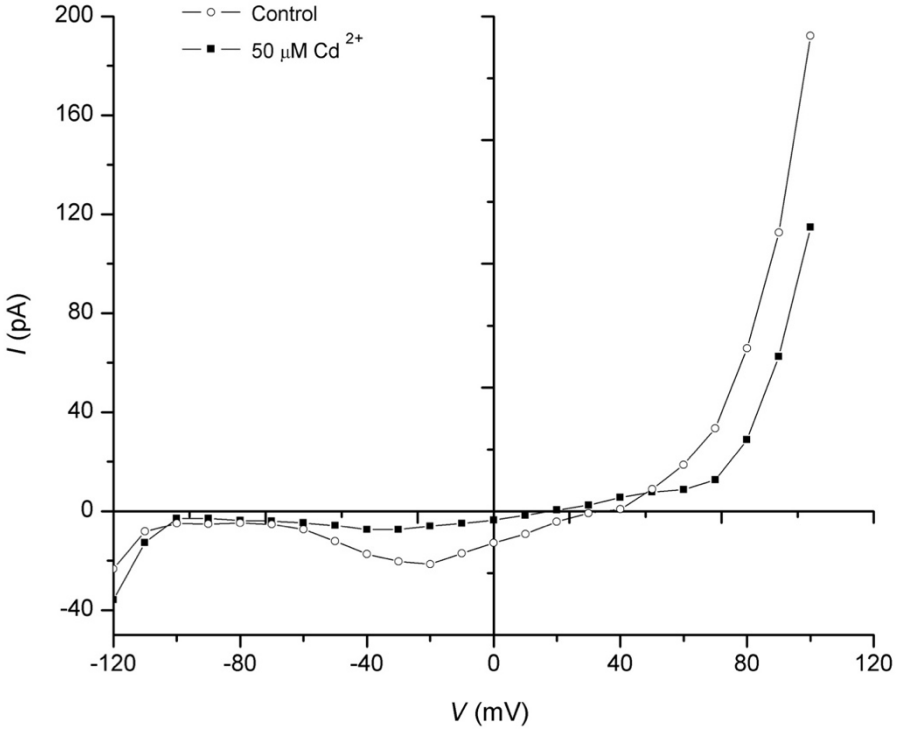
Control
50 µM Cd 2+
200
160
120
80
40
0
-40
I (pA)
-120
-80
-40
0
40
80
120
V (mV)

Figure 5. I-V relationship of calcium currents in hypoxia and normoxia

A, Voltage-clamp recording in a cell stepped from a voltage of -60 mV to various voltages (see figure) in control, hypoxia and after wash. ***B***, I-V relationship of the recordings from the cell in *A* demonstrates activation of calcium currents at approximately -40 mV, with a peak current at 10 mV. A slight increase in calcium current under hypoxia was seen in this cell. Run-down of K_{ir} can also be seen as the I-V curve progresses from control to wash. ***C,*** enlarged I-V curve of currents in *B* highlighting a slight increase in calcium, from around 25 to 40 pA at voltage +10mV, under hypoxia in comparison to normoxia (control). Calcium current partially recovered upon administration of the wash solution.

A

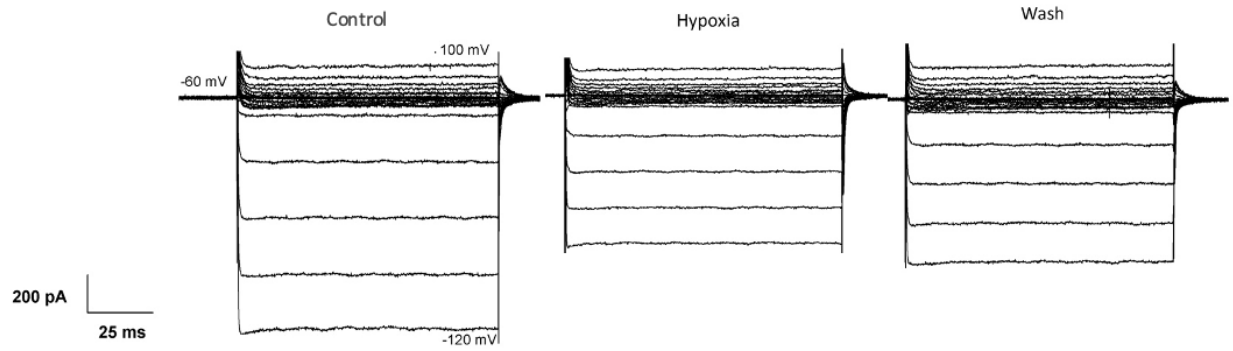
Control
Hypoxia
Wash
100 mV
-60 mV
-120 mV
200 pA
25 ms

B

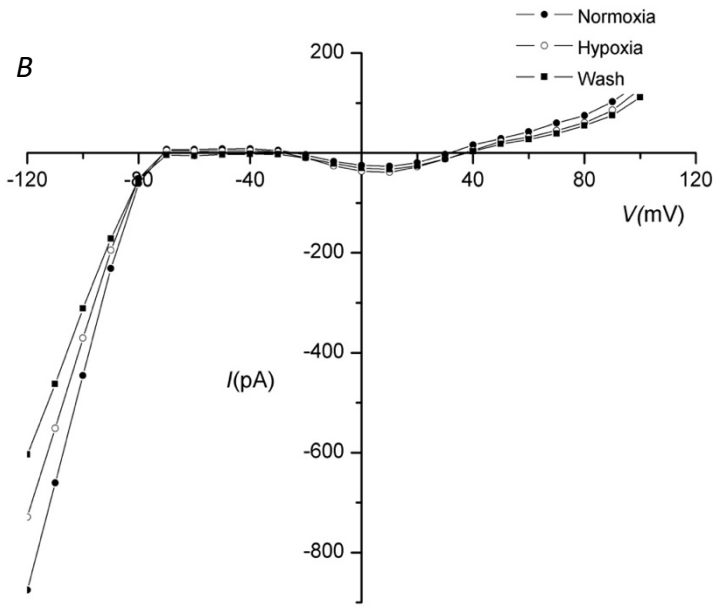
Normoxia
Hypoxia
Wash
200
-200
-400
-600
-800
-120
-80
-40
40
80
120
V(mV)
I(pA)

C

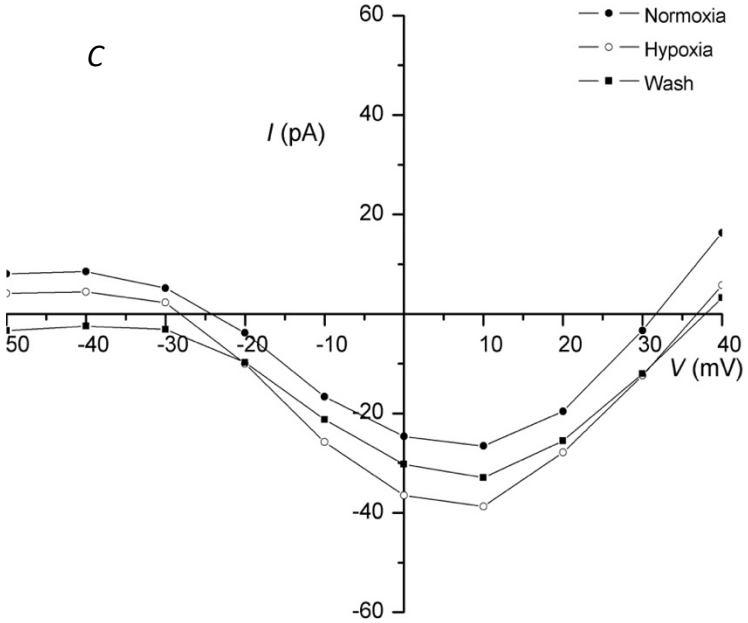
Normoxia
Hypoxia
Wash
60
40
20
-20
-40
-60
50
-40
-30
-20
-10
10
20
30
40
I (pA)
V (mV)

Figure 6. Calcium currents were not significantly increased by hypoxia

Summary data of HC ion currents plotted as current density (pA/pF) in normoxia, hypoxia and wash (n=3). Values are presented as the mean with the interquartile range. The figure shows a slight increase in calcium currents during hypoxia in two cells, and one cell did not show an increase. No significance was found in comparison to control values ($P>0.05$; Freidman test)

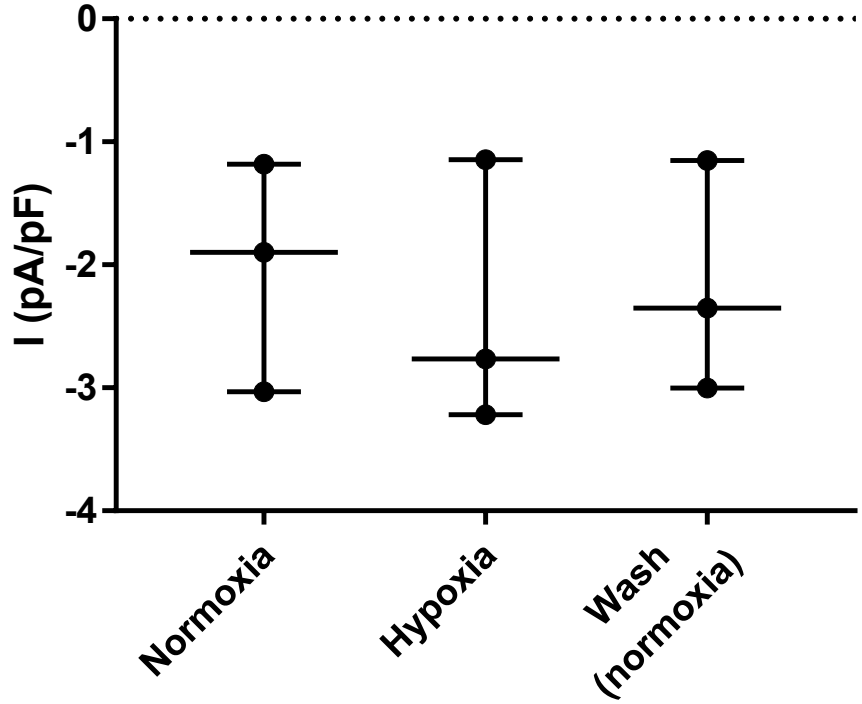
0
-1
-2
-3
-4
I (pA/pF)
Normoxia
Hypoxia
Wash
(normoxia)

Discussion

This study has described the potential effects of hypoxia on various currents in horizontal cells (HCs) of the goldfish retina. I have demonstrated that hypoxia increases glutamate-activated currents and have introduced hypoxia's potential increasing effect on Ca^{2+} channel currents.

Horizontal cells of the retina express multiple types of ionotropic glutamate receptors, including NMDA, AMPA and kainate receptors, but namely AMPA-type ionotropic glutamate receptors (Brandstätter et al., 1998). When the retina is exposed to darkness or low light conditions, pre-synaptic photoreceptors are relatively depolarized and tonically release glutamate onto second-order neurons, such as horizontal cells and bipolar cells (Thoreson & Mangel, 2012). Their activation by glutamate elicits multiple changes in membrane conductance. These changes include inhibiting K_{ir} channels, suppressing Ca^{2+} channels, and enhanced outward rectification (Kaneko & Tachibana, 1985; Tachibana, 1985; Dixon *et al*. 1993). The present study has replicated modulation of the previously described inward and outward current characteristics by applying glutamate in isolated goldfish HCs, specifically in normoxia and hypoxia. Based on unpublished Ca^{2+} imaging data from this lab (Nagy, unpublished), it has been shown that isolated HCs of the goldfish retina display significant increases in $[Ca^{2+}]_i$ upon glutamate activation in hypoxia. Therefore, we hypothesized that using whole-cell patch-clamp techniques, we might produce data that complements these preliminary findings.

In the present experiments, hypoxia induced an increase in the glutamate-activated current, which is carried primarily by Na^+ through AMPA receptors (Country et al., 2017). Using whole-cell patch-clamp techniques, the voltage in these experiments was clamped for milliseconds at a time at voltages ranging from -120 to 100 mV. Since voltages were clamped, we were unable to observe the spontaneous activity of HCs and spontaneous depolarization of the membrane.

However, we can imagine that an increase in Na^+ influx through AMPA receptors will likely further depolarize HCs.

Currently, the specific role that excess Na^+ influx might play in isolated HCs is unclear. Though, it should be noted that in the context of *in vivo* systems, any depolarization of HCs will elicit further inhibition onto presynaptic PRs, resulting in the closure of VGCCs and reduction of glutamate release from PRs (Vessey et al., 2005; Thoreson and Mangel, 2012). Tonic release of glutamate by PRs is an energetically costly process since ATP consumption is significantly increased in darkness when photoreceptors are depolarized (Xu et al., 2007). To prevent this energy expenditure when ATP supply is already limited, hypoxia may induce a neuroprotective mechanism in PRs by downregulating their release of glutamate. To extend this model further, a reduction of glutamate release from photoreceptors may subsequently limit AMPA receptor activation on post-synaptic neurons, effectively hyperpolarizing bipolar and horizontal cells during hypoxia and limiting energy consumption. Since this is mere speculation of a neuroprotective mechanism, it will be important for future studies to test these hypotheses in retinal slice preparations (Vessey et al., 2005; Country et al., 2021), where synaptic contacts between photoreceptors and other neurons are preserved and the effects of hypoxia on feedback can be properly assessed *in situ*.

Although I have described a hypothesis for what might be taking place in the retina during hypoxia, it remains unclear *how* increased current through glutamate receptors might occur at the molecular level. It is possible that hypoxia is directly acting on the glutamate receptors themselves, or perhaps acting indirectly by modulation of the voltage across the plasma membrane. Some studies that have looked at the effects of hypoxia on glutamate receptors have shown the opposite effects of what we have shown in isolated HCs. For example, a study conducted by Wilkie and

colleagues showed induced channel arrest of NMDA receptors under anoxic conditions, and as a result, prevented potentially excitotoxic effects in neurons of the goldfish brain (Wilkie *et al.*, 2008). It can be argued then that though previous studies have shown channel arrest as opposed to increased channel activity, perhaps the described mechanism of channel arrest does not apply to the goldfish retina as it does to the brain. Based on our results, we suspect that glutamate receptor activation might be involved in neuroprotection.

An additional explanation for the proposed depolarization in hypoxia aligns with the phenomenon of "anoxic depolarization", where low oxygen conditions induce extreme depolarization in neurons. There is evidence that this occurs *in vivo* and in retinal slices; however, there has not been evidence of this in isolated cells as of yet. The molecular basis for anoxic depolarization has not been solidified, though there is strong evidence that depolarization arises from inhibiting the Na^+/K^+-ATPase pump (Lipton, 1999). Additionally, HCs are connected via hemichannels and thus exhibit hemichannel currents (Klaassen *et al.*, 2011). Increased opening of these channels may also contribute to the basis of anoxic depolarization by ionic dysregulation in low oxygen (Thompson *et al.*, 2006).

To add to this model of increased depolarization, as mentioned, it has been suggested that isolated HCs of the goldfish retina *may* show significant increases in $[Ca^{2+}]_i$ upon glutamate activation in hypoxia (Nagy, unpublished). The increased Ca^{2+} influx may occur upon increased depolarization of HCs, and thus might play a key role in this possible protective effect. In the context of calcium-dependent depolarization (via L-type Ca^{2+} channels or through GluRs), any additional Ca^{2+} influx might increase the release of GABA from HCs (Barnes et al., 2020). This increased release of inhibitory neurotransmitters will subsequently inhibit photoreceptors, potentially via a combined GABA-pH model of inhibition. In this model, the depolarization of the

HC causes GABA to release which activates GABA auto receptors embedded in the HC membrane. The result is a buffering in pH at the synaptic cleft which modulates photoreceptor transmitter release via surface charge effects on the VGCCs of presynaptic PRs (Barnes et al., 1993; Vessey et al., 2005).

In the present study, characteristics of Ca^{2+} channels alone were also investigated in hypoxia. As previously mentioned, Ca^{2+} plays a very important role in the onset of excitotoxicity, leading to apoptosis. In non-hypoxia-tolerant species, low oxygen will induce an increase in Ca^{2+} levels which become toxic to the cell. Based on the notion that *C. auratus* has been shown to regulate intracellular Ca^{2+} levels during extended periods of hypoxia (Country et al. 2021), the rationale for studying the membrane physiology of Ca^{2+} channels in hypoxia is justified. In this study, I noticed a slight increase in Ca^{2+} currents through voltage-gated channels in hypoxia. Due to time constraints and difficulties with data collection, data were collected from only 3 cells. Further studies might aim to better isolated Ca^{2+} current by blocking other channels (e.g. K_{ir} channels) to confirm whether hypoxia has an effect on Ca^{2+} channels.

The increased activity of Ca^{2+}-permeable glutamate receptors, and increase Ca^{2+} current that were measured in 2 of the 3 cells observed, are reminiscent of the "paradoxical" increase in $[Ca^{2+}]_i$ previously described in neurons of the western painted turtle. In this model, hypoxia increased intracellular Ca^{2+} which accumulated and regulated the activity of the NMDA receptors (Pamenter *et al.*, 2008). It can be postulated then that the increase we have shown in the present study may be similar, where the increase in Ca^{2+} is a mechanism of neuroprotection for the cell. It should be noted that our results differ in that we have shown an increase in glutamate receptor activation, as opposed to a decrease. However, perhaps in the goldfish retina, the role of increased Ca^{2+} is not to modulate glutamate receptors, but to modulate photoreceptors by increased depolarization of HCs.

Although there is evidence that points to a slight increase in Ca^{2+}, horizontal cells are quite efficient at buffering intracellular Ca^{2+} compared to other neurons (Country et al., 2017), so a small rise in Ca^{2+} may not pose too much of a threat to HCs. This lab has recently demonstrated a mechanism involving mKATP channels in HCs of goldfish that may protect against an increase in intracellular Ca^{2+} and help to maintain homeostasis (Country and Jonz 2021). Another preliminary finding from this lab suggests that a hypoxic increase in intracellular Ca^{2+} is dependent upon mKATP (Nagy, unpublished), suggesting that mKATP might be involved in two protective pathways during hypoxia: one being the maintenance of low intracellular Ca^{2+} levels in unstimulated HCs (Country and Jonz 2021), and another that induces membrane depolarization by way of glutamate-induced depolarization. Further study will need to be conducted to understand the role of mKATP in Ca^{2+} regulation.

Our results showed instances of Ca^{2+} current increase; however, these increases were not very large and most likely would not be harmful to the cell in the way excitotoxicity might be. The first-order synapse between PRs and HCs is unique in that there is very little space between them, resulting in the low availability of extracellular Ca^{2+} in the synaptic space. Additionally, there are a limited number of Ca^{2+} channels alone to support tonic release of glutamate from PRs (Rabl & Thoreson, 2002). Due to this limited amount of Ca^{2+} in the space between HCs and PRs, if either glutamate receptors or Ca^{2+} channels were to allow increased Ca^{2+} influx during hypoxia *in vivo,* there may not be much Ca^{2+} that gets into the cell because of this decreased Ca^{2+} availability is the extracellular space. Although the influx of Ca^{2+} is not expected to be drastic, even a small increase in Ca^{2+} influx from the extracellular space would be enough to contribute to increased GABA release in the novel neuroprotective mechanism I have described.

Overall, much more work needs to be done to understand the mechanisms used by HCs to withstand hypoxic conditions. But we may have described a novel mechanism whereby depolarization and increased Ca^{2+} currents are key players in the inhibition of other neurons (e.g. photoreceptors).

Conclusion

Using whole-cell patch-clamp electrophysiology, this study has shown the effect of hypoxia on ion channel currents in isolated HCs of the goldfish retina. Administration of hypoxic solution led to an increase in glutamate-activated currents in isolated HCs. Although preliminary and based on a small sample size, the evidence presented suggests that currents through voltage-dependent Ca^{2+} channels may also have increased during hypoxic exposure. These findings may represent parts of a neuroprotective mechanism in the retina by which hypoxia increases glutamate-activated inward currents, leading to depolarization of HCs and subsequent feedback inhibition of pre-synaptic PRs to limit ATP consumption. Increased intracellular Ca^{2+}, through glutamate receptors or Ca^{2+} channels, may further contribute to inhibitory feedback by enhancing GABA release from HCs. Further investigation is required to understand how glutamate currents are increased by hypoxia in these cells. Future studies may also determine the effects of hypoxia on Ca^{2+} currents since our data is preliminary in this regard. This research will contribute to the story of how the retina is protected in hypoxia-tolerant vertebrates exposed to prolonged oxygen deprivation. Further, the findings of this study may provide new insights into reducing or preventing retinal diseases and stroke, which are commonly caused by cell death due to ischemia (Osborne et al., 2004; Hayreh & Zimmerman, 2005).

References

Ames A (2011). Energy requirements of CNS cells as related to their function and to their vulnerability to ischemia: a commentary based on studies on retina. *https://doi.org/101139/y92-257*; DOI: 10.1139/Y92-257.

Ankri L, Ezra-Tsur E, Maimon SR, Kaushansky N & Rivlin-Etzion M (2020). Antagonistic Center-Surround Mechanisms for Direction Selectivity in the Retina. *Cell Reports* 31, 107608.

Armada-Moreira A, Gomes JI, Pina CC, Savchak OK, Gonçalves-Ribeiro J, Rei N, Pinto S, Morais TP, Martins RS, Ribeiro FF, Sebastião AM, Crunelli V & Vaz SH (2020). Going the Extra (Synaptic) Mile: Excitotoxicity as the Road Toward Neurodegenerative Diseases. Frontiers in Cellular Neuroscience 14, 90.

Barnes S, Grove JCR, McHugh CF, Hirano AA & Brecha NC (2020). Horizontal Cell Feedback to Cone Photoreceptors in Mammalian Retina: Novel Insights From the GABA-pH Hybrid Model. Frontiers in Cellular Neuroscience 14, 341.

Barnes S, Merchant V & Mahmud F (1993). Modulation of transmission gain by protons at the photoreceptor output synapse. Proc Natl Acad Sci U S A 90, 10081–10085.

Beckwith-Cohen B, Holzhausen LC, Wang TM, Rajappa R & Kramer RH (2019). Localizing Proton-Mediated Inhibitory Feedback at the Retinal Horizontal Cell–Cone Synapse with Genetically-Encoded pH Probes. Journal of Neuroscience 39, 651–662.

Berliocchi L, Bano D & Nicotera P (2005). Ca2 signals and death programmes in neurons. Philosophical Transactions of the Royal Society B: Biological Sciences 360, 2255–2258.

Bhangoo SK & Swanson GT (2013). Kainate Receptor Signaling in Pain Pathways. Molecular Pharmacology 83, 307.

Bickler PE & Buck LT (1998). Adaptations of vertebrate neurons to hypoxia and anoxia: maintaining critical Ca2+ concentrations. Journal of Experimental Biology 201, 1141–1152.

Bickler PE & Buck LT (2007). Hypoxia tolerance in reptiles, amphibians, and fishes: life with variable oxygen availability. Annu Rev Physiol 69, 145–170.

Brandstätter JH, Koulen P & Wässle H (1998). Diversity of glutamate receptors in the mammalian retina. Vision Research 38, 1385–1397.

Byzov AL & Shura-Bura TM (1986). Electrical feedback mechanism in the processing of signals in the outer plexiform layer of the retina. Vision Res 26, 33–44.

Byzov AL & Trifonov JA (1968). The response to electric stimulation of horizontal cells in the carp retina. Vision Res 8, 817–822.

Connaughton VP & Dowling JE (1998). Comparative morphology of distal neurons in larval and adult zebrafish retinas. Vision Res 38, 13–18.

Country MW, Jonz MG (2017). Calcium dynamics and regulation in horizontal cells of the vertebrate retina: lessons from teleosts. *J Neurophysiol* **117,** 523–536.

Country MW, Jonz MG (2021). Mitochondrial KATP channels stabilize intracellular Ca2+ during hypoxia in retinal horizontal cells of goldfish (Carassius auratus). *J Exp Biol*; DOI: 10.1242/JEB.242634.

Dixon DB, Takahashi KI & Copenhagen DR (1993). L-glutamate suppresses HVA calcium current in catfish horizontal cells by raising intracellular proton concentration. *Neuron* **11,** 267–277.

Dong X-X, Wang Y & Qin Z-H (2009). Molecular mechanisms of excitotoxicity and their relevance to pathogenesis of neurodegenerative diseases. Acta Pharmacologica Sinica 30, 379–387.

Dowling JE (1987). The retina: an approachable part of the brain. Harvard University Press

Feher J (2012). Vision. Quantitative Human Physiology456–470.

Filice M, Mazza R, Leo S, Gattuso A, Cerra MC & Imbrogno S (2020). The Hypoxia Tolerance of the Goldfish (Carassius auratus) Heart: The NOS/NO System and Beyond. Antioxidants 9, 1–16.

Gasbarri A & Pompili A (2014). Involvement of Glutamate in Learning and Memory. Identification of Neural Markers Accompanying Memory63–77.

Haverkamp S, Wa¨ssle H & Wa¨ssle W (2000). Immunocytochemical Analysis of the Mouse Retina. J Comp Neurol 424, 1–23.

Hayashida Y & Yagi T (2002). Contribution of Ca2+ transporters to electrical response of a non-spiking retinal neuron. *Neurocomputing* **44–46,** 7–12.

Hayreh SS & Zimmerman MB (2005). Central retinal artery occlusion: visual outcome. *Am J Ophthalmol* **140,** 376.e1-376.e.

Hermes-Lima M & Zenteno-Savín T (2002). Animal response to drastic changes in oxygen availability and physiological oxidative stress. *Comp Biochem Physiol C Toxicol Pharmacol* **133,** 537–556.

Hochachka PW (1986). Defense strategies against hypoxia and hypothermia. *Science* **231,** 234–241.

Hoon M, Okawa H, della Santina L & Wong ROL (2014). Functional Architecture of the Retina: Development and Disease. *Prog Retin Eye Res* **42,** 44.

Jacoby J, Kreitzer MA, Alford S, Qian H, Tchernookova BK, Naylor ER & Malchow RP (2012). Extracellular pH dynamics of retinal horizontal cells examined using electrochemical and fluorometric methods. *Journal of Neurophysiology* **107,** 868.

Johansson D, Nilsson GE & Døving KB (1997). Anoxic depression of light-evoked potentials in retina and optic tectum of crucian carp. *Neurosci Lett* **237,** 73–76.

Jonz MG & Barnes S (2007). Proton modulation of ion channels in isolated horizontal cells of the goldfish retina. *The Journal of Physiology* **581,** 529.

Kaneko A (1971). Electrical connexions between horizontal cells in the dogfish retina. *J Physiol* **213,** 95–105.

Keenan SW, Hill CA, Kandoth C, Buck LT & Warren DE (2015). Transcriptomic Responses of the Heart and Brain to Anoxia in the Western Painted Turtle. *PLOS ONE* **10,** e0131669.

Klaassen LJ, Sun Z, Steijaert MN, Bolte P, Fahrenfort I, Sjoerdsma T, Klooster J, Claassen Y, Shields CR, ten Eikelder HMM, Janssen-Bienhold U, Zoidl G, McMahon DG & Kamermans M (2011). Synaptic Transmission from Horizontal Cells to Cones Is Impaired by Loss of Connexin Hemichannels. *PLoS Biology* **9,** 1001107.

Kramer RH & Davenport CM (2015). Lateral Inhibition in the Vertebrate Retina: The Case of the Missing Neurotransmitter. *PLoS Biology*; DOI: 10.1371/JOURNAL.PBIO.1002322.

Lipton P (1999). *Ischemic Cell Death in Brain Neurons*.

Mehta A, Prabhakar M, Kumar P, Deshmukh R & Sharma PL (2013). Excitotoxicity: bridge to various triggers in neurodegenerative disorders. *Eur J Pharmacol* **698,** 6–18.

Nilsson GE (2001). Surviving anoxia with the brain turned on. *News in Physiological Sciences* **16,** 217–221.

O'Brien JJ, Li W, Pan F, Keung J, O'Brien J & Massey SC (2006). Coupling between A-Type Horizontal Cells Is Mediated by Connexin 50 Gap Junctions in the Rabbit Retina. *The Journal of Neuroscience* **26,** 11624.

Osborne NN, Casson RJ, Wood JPM, Chidlow G, Graham M & Melena J (2004). Retinal ischemia: mechanisms of damage and potential therapeutic strategies. *Prog Retin Eye Res* **23,** 91–147.

Pál B, Pankratov Y, Valentino M, Anderova M, Kirdajova BD, Belov Kirdajova D, Kriska J & Tureckova J (2020). Ischemia-Triggered Glutamate Excitotoxicity From the Perspective of Glial Cells. ; DOI: 10.3389/fncel.2020.00051.

Palmer CL, Cotton L & Henley JM (2005). The Molecular Pharmacology and Cell Biology of α-Amino-3-hydroxy-5-methyl-4-isoxazolepropionic Acid Receptors. *Pharmacol Rev* **57,** 253.

Pamenter ME, Shin DSH, Cooray M & Buck LT (2008). Mitochondrial ATP-sensitive K+ channels regulate NMDAR activity in the cortex of the anoxic western painted turtle. *J Physiol* **586,** 1043–1058.

Papazian I, Kyrargyri V, Evangelidou M, Voulgari-Kokota A & Probert L (2018). Mesenchymal Stem Cell Protection of Neurons against Glutamate Excitotoxicity Involves Reduction of NMDA-Triggered Calcium Responses and Surface GluR1, and Is Partly Mediated by TNF. *International Journal of Molecular Sciences 2018, Vol 19, Page 651* **19,** 651.

Perlman I, Kolb H, and Nelson R (2011). S-potentials and horizontal cells. Webvision: the organization of the retina and visual system [Internet] Salt Lake City (UT): University of Utah Health Sciences Center

Poché RA & Reese BE (2009). Retinal horizontal cells: challenging paradigms of neural development and cancer biology. *Development* **136,** 2141.

del Prete D, Checler F & Chami M (2014). Ryanodine receptors: physiological function and deregulation in Alzheimer disease. *Mol Neurodegener*; DOI: 10.1186/1750-1326-9-21.

Rabl K & Thoreson WB (2002). Calcium-dependent inactivation and depletion of synaptic cleft calcium ions combine to regulate rod calcium currents under physiological conditions. *Eur J Neurosci* **16,** 2070–2077.

Sakai HM & Naka K -I (1986). Synaptic organization of the cone horizontal cells in the catfish retina. *J Comp Neurol* **245,** 107–115.

Schmitz F (2009). The making of synaptic ribbons: how they are built and what they do. *Neuroscientist* **15,** 611–624.

Shekhar K, Lapan SW, Whitney IE, Tran NM, Macosko EZ, Kowalczyk M, Adiconis X, Levin JZ, Nemesh J, Goldman M, McCarroll SA, Cepko CL, Regev A & Sanes JR (2016). COMPREHENSIVE CLASSIFICATION OF RETINAL BIPOLAR NEURONS BY SINGLE-CELL TRANSCRIPTOMICS. *Cell* **166,** 1308.

Shingai R & Christensen BN (1986). Excitable properties and voltage-sensitive ion conductances of horizontal cells isolated from catfish (Ictalurus punctatus) retina. J Neurophysiol **56**, 32–49

Snellman J, Kaur T, Shen Y & Nawy S (2008). Regulation of ON Bipolar Cell Activity. *Prog Retin Eye Res* **27,** 450.

Stell WK & Lightfoot DO (1975). Color-specific interconnections of cones and horizontal cells in the retina of the goldfish. *J Comp Neurol* **159,** 473–501.

Ströh S, Puller C, Swirski S, Hölzel M-B, Lea X, van der Linde IS, Segelken XJ, Schultz K, Block C, Monyer H, Willecke K, Weiler X, Greschner M, Janssen-Bienhold U & Dedek K (2018). Eliminating Glutamatergic Input onto Horizontal Cells Changes the Dynamic Range and Receptive Field Organization of Mouse Retinal Ganglion Cells. *Journal of Neuroscience* **38,** 2015–2028.

Svaetichin G (1953). The cone action potential. *Acta physiol scand* 29: 565-599

Tachibana M (1983). Ionic currents of solitary horizontal cells isolated from goldfish retina. *The Journal of Physiology* **345,** 329.

Tachibana M (1985). Permeability changes induced by L-glutamate in solitary retinal horizontal cells isolated from Carassius auratus. *J Physiol* **358,** 153–167.

Takahashi KI, Dixon DB & Copenhagen DR (1993). Modulation of a sustained calcium current by intracellular pH in horizontal cells of fish retina. *J Gen Physiol* **101,** 695–714.

Thompson RJ, Zhou N & MacVicar BA (2006). Ischemia opens neuronal gap junction hemichannels. *Science* **312,** 924–927.

Thoreson WB & Mangel SC (2012). Lateral interactions in the outer retina. *Progress in Retinal and Eye Research* **31,** 407.

Twomey EC & Sobolevsky AI (2018). Structural Mechanisms of Gating in Ionotropic Glutamate Receptors. *Biochemistry* **57,** 267–276.

Vessey JP, Stratis AK, Daniels BA, da Silva N, Jonz MG, Lalonde MR, Baldridge WH & Barnes S (2005). Proton-mediated feedback inhibition of presynaptic calcium channels at the cone photoreceptor synapse. *J Neurosci* **25,** 4108–4117.

Wässle H (2004). Parallel processing in the mammalian retina. *Nature Reviews Neuroscience 2004 5:10* **5,** 747–757.

Wilkie MP, Pamenter ME, Alkabie S, Carapic D, Shin DSH & Buck LT (2008). Evidence of anoxia-induced channel arrest in the brain of the goldfish (Carassius auratus). *Comp Biochem Physiol C Toxicol Pharmacol* **148,** 355–362.

Xu Y, Ola MS, Berkich DA, Gardner TW, Barber AJ, Palmieri F, Hutson SM & LaNoue KF (2007). Energy sources for glutamate neurotransmission in the retina: absence of the aspartate/glutamate carrier produces reliance on glycolysis in glia. *J Neurochem* **101,** 120–131.

Yang XL & Wu SM (1991). Feedforward lateral inhibition in retinal bipolar cells: input-output relation of the horizontal cell-depolarizing bipolar cell synapse. *Proc Natl Acad Sci U S A* **88,** 3310.

Yin Shen, Xiao-Ling Liu & Xiong-Li Yang (2006). *N-Methyl-D-Aspartate Receptors in the Retina*.